Ab Initio Study of the Electronic Structure and Bonding of Aluminum Nitride†

Apostolos Kalemos* and Aristides Mavridis*

Laboratory of Physical Chemistry, Department of Chemistry, National and Kapodistrian University of Athens, P.O. Box 64 004, 157 10 Zografou, Athens, Greece

Received: January 22, 2007; In Final Form: February 21, 2007

For the diatomic aluminum nitride (AlN), we have constructed potential energy curves for 45 states employing multi-reference variational methods and quantitative basis sets. Thirty-six states are relatively strongly bound, five present local minima, and four are of repulsive nature. Almost all states are of intense multi-reference character rendering their calculation and interpretation quite problematic. Our tentative assignment of the ground state is $^3\Pi$, while a $^3\Sigma^-$ state is above by less than 1 kcal/mol. Our best estimate for the binding energy of the $X^3\Pi$ state is $D_0 = 56.0 \pm 0.5$ kcal/mol at $r_e = 1.783$ Å, in good agreement with the experimental values of $D = 66 \pm 9$ kcal/mol and $r_e = 1.7864$ Å. The binding energy of the $A^3\Sigma^-$ state is very similar to the X state because they both correlate to the ground-state atoms, but the bond distance of the former is 0.13 Å longer. The first seven states can be tagged as follows: $X^3\Pi$, $A^3\Sigma^-$, $a^1\Sigma^+$, $b^1\Pi$, $c^1\Delta$, $B^3\Sigma^+$, and $d^1\Sigma^+$, a rather definitive order with the exception of X and A states.

1. Introduction

The first experimental study on aluminum nitride (AlN), the second-row analog of BN, was performed using emission spectroscopy by Simmons and McDonald in 1972.[1] Two bands were recorded, a strong one at 5078 Å and a much weaker at 5276 Å, assigned to the $v' = 0 \rightarrow v'' = 0$ and $v' = 0 \rightarrow v'' = 1$ lines of a $^3\Pi \rightarrow {}^3\Pi$ transition. The analysis of the bands' characteristics gave, $\nu(0-0) = 19{,}727.37 \pm 0.03$ ($19{,}727.13 \pm 0.06$) cm^{-1} and $\nu(0-1) = 18{,}980.44 \pm 0.06$ cm^{-1} for $Al^{14}N$-($Al^{15}N$). Despite their efforts, no trace of the $v' = 1 \rightarrow v'' = 0$ transition was detected.

Twenty years later, Ebben and ter Meulen succeeded in observing the $v' = 1(C^3\Pi) \rightarrow v'' = 0(X^3\Pi)$ transition by laser-induced fluorescence spectroscopy.[2] They obtained the following spectroscopic constants (in cm^{-1}): $\nu(1-0) = 20\,484.71 \pm 0.03$, $\Delta G_{1/2}' = 757.39$, $\omega_e' = 779.4$, $\omega_e x_e' = 11.0$, and $T_e = 19{,}718.1$, whereas from the data of Simmons and McDonald[1] they extracted $\omega_e'' = 758.4$, $\omega_e x_e'' = 5.7$, and $\Delta G_{1/2}'' = 746.93$.

The first theoretical treatment on AlN was published in 1979 by Pelissier and Malrieu.[3] Using the HF orbitals of the lowest closed shell $^1\Sigma^+$ state and pseudopotentials to represent the cores, these authors constructed potential energy curves (PEC) at the CIPSI (configuration interaction by perturbation with multi-configurational zeroth-order wavefunction selected by iterative process) level of theory for the $X^3\Pi$ state and five additional states of $^{1,3}\Pi$, $^{1,3}\Sigma^+$, and $^3\Sigma^-$ symmetry (see Table 1).

The most elaborate theoretical study until now is that of Langhoff et al., published almost 20 years ago.[4] By using large ANO basis sets ([6s5p2d1f/$_{Al}$ 5s4p2d1f/$_N$]) and multi-reference configuration interaction techniques (MRCI), they constructed the PECs of eight AlN states, whereas within the complete active space self-consistent field (CASSCF) approach, they calculated the transition and radiative life times of dipole allowed transitions. According to these workers the ground state of AlN is probably of $^3\Pi$ symmetry with a $^3\Sigma^-$ state about 1 kcal/mol higher. The dissociation energy of the $X^3\Pi$ was calculated to be D_e(MRCI) = 2.20 eV (= 50.73 kcal/mol).

In 1999, Gutsev et al.[5] studied the structure and stability of the $^3\Pi$,$^3\Sigma^-$,$^3\Sigma^+$, and $^1\Sigma^+$ AlN states by coupled-cluster (CCSD-(T)/[7s7p5d4f/$_{Al}$7s7p4d3f/$_N$]) methods. The $^3\Sigma^-$ state was found to be lower than the $^3\Pi$ by 21 cm^{-1} (Table 1).

A MRDCI study of the $^{1,3}\Pi$,$^3\Sigma^-$,$^1\Sigma^+(2)$,$^3\Sigma^+$, and $^1\Delta$ states appeared in 2003.[6] The ground state was determined to be of $^3\Pi$ symmetry, about 160 cm^{-1} lower that the $^3\Sigma^-$ state (Table 1). In 2005 another CCSD(T) study of the $^3\Pi$, $^3\Sigma^-$, and $^1\Sigma^+$ states showed that $^3\Pi$ and $^3\Sigma^-$ are practically degenerate,[7] with the former being lower by 155 cm^{-1}. The most recent *ab initio* study that we are aware of is by Gan et al.,[8] who by CCSD(T) and full-CI (FCI) methods studied the $^3\Pi$, $^3\Sigma^-$, and $^1\Sigma^+$ states of the isovalent series of molecules BN, BP, AlN, and AlP. At the FCI/cc-pVTZ level the $^3\Pi$ is lower than the $^3\Sigma^-$ by just 37.6 cm^{-1} (Table 1).

A number of density functional theory (DFT) studies on AlN have also appeared, the results of which are included in Table 1 for reasons of completeness.[9] Practically, all existing information on AlN has been collected in Table 1. Notice that two experimental dissociation energies are available for the (formal) ground state $^3\Pi$[10,11] and one for the second excited-state $a^1\Sigma^+$.[12] Meloni and Gingerich by Knudsen cell mass spectrometry obtained $D(X^3\Pi) \leq 87.63 \pm 3.69$ kcal/mol,[10] which even as an upper bound value is certainly overestimated (*vide infra*), whereas the value of ref 11, $D = 66 \pm 9$, is more realistic.

From the short exposition above, it is rather evident that a more systematic and accurate study on AlN is needed; the aim of the present study is to fill this gap. By employing the MRCI methodology and large basis sets, we have constructed 45 PECs: 36 bound and 3 of Rydberg character. The present work will also serve as the first step for the study of the triatomic AlNAl system, isovalent to BNB[13] and "prone" to symmetry-breaking effects due to its bonding structure and according to recent experimental data.[14]

† Part of the "Thom H. Dunning, Jr., Festschrift".

* Corresponding authors. E-mail: mavridis@chem.uoa.gr and kalemos@chem.uoa.gr.

10.1021/jp070544o CCC: $37.00
Published on Web 04/27/2007

TABLE 1: Existing Theoretical and Experimental Data on AlN[a]

$-E$	r_e	D_e	$\omega_e/\omega_e x_e$	T_e	reference
		$X^3\Pi$			
	1.83	55.75	772.0/4.6	0	3[b]
	1.814(1.818)	50.73(54.19)	746(738)	+300(0)	4[c]
	1.816(1.817)		742(737)	+420(0)	4[d]
	1.80(1.78)	64.11(81.64)			9a[e]
296.721 178	1.7909	56.50	756	+20.63	5[f]
	1.805(1.821)	60	730(717)		9b[g]
	1.82	63.19	710		9c[h]
	1.79	70.11			9d[i]
	1.805	66.19	752		9e[j]
296.5261(MO)	1.808(MO)	53.50	734/6.8(MO)	0	6[k]
296.5298(NO)	1.814(NO)		718/6.9(NO)	0	6[k]
297.0794	1.800		743.4		9f[l]
296.549 580	1.8031	57.07(= D_0)	745.06/5.65	+154.95	7[m]
296.530 4629		52.59		0	8[n]
	1.7908(= r_0)				1, expt.[o]
	1.7864		758.4/5.7		2, expt.[p]
		$\leq 87.63 \pm 3.69$			10, expt.[q]
		65.95 ± 8.99			11, expt.
		$A^3\Sigma^-$			
	1.89	47.46	806.0/5.0	2933	3[b]
	1.936(1.949)		637(587)	0(+99)	4[c]
	1.942(1.944)		604(582)	0(+378)	4[d]
296.721 272	1.9156		628	0	5[f]
	1.930		622/5.2	161.31	6[k]
296.550 286	1.9287	57.26	622.54/4.54	0	7[m]
296.530 2916				37.60	8[n]
		$a^1\Sigma^+$			
	1.70	109.79	994.0/4.8	1270	3[b]
	1.693(1.694)		919(913)	4640(4689)	4[c]
296.705 968	1.6667		985	3358.84	5[f]
	1.688	93.17	940		9e[j]
	1.683		989/9.3	3952.19	6[k]
296.535 471	1.6771	47.78(= D_0)	970.7/6.04	3251.52	7[m]
296.511 1857				4230.86	8[n]
	1.65	87.22	930/6.5		12, expt.
		$b^1\Pi$			
	1.78	91.21	869.0/6.9	6543	3[b]
	1.786(1.785)		796(794)	6517(6186)	4[c]
	1.778		863/8.3	6210.59	6[k]
		$c^1\Delta$			
	1.926(1.942)		656(605)	10723(10754)	4[c]
	1.914		576/0.12	11614.61	6[k]
		$B^3\Sigma^+$			
	1.68	87.49	1267.0/6.9	9021	3[b]
	1.679(1.676)		905(907)	15537(15445)	4[c]
296.652 871	1.6366		1070	15012.29	5[f]
	1.666		962/7.7	14356.95	6[k]
		$2^1\Sigma^+$			
	1.885		725/3.0	18067.17	6[k]
		$C^3\Pi$			
	1.74	43.74	1041.0/4.9	23095	3[b]
	1.807(1.809)		720(722)	19310(19011)	4[c]
			779.4/11.0	19718.1	2, expt.[p]
	1.7739(= r_0)			19727.37 ± 0.03	1, expt.[o]
		$e^1\Pi$			
	1.902(1.920)		607/583	24508(24511)	4[c]

[a] Total energies E (E_h), bond distances r_e (Å), dissociation energies D_e (kcal/mol), harmonic and anharmonic frequencies $\omega_e/\omega_e x_e$ (cm^{-1}), and energy separations T_e (cm^{-1}). [b] CI(CIPSI) calculations based on HF orbitals of the $a^1\Sigma^+$ state, pseudopotentials + DZP. [c] MRCI(0.05)/[6s5p2d1f/5s4p2d1f]; Davidson corrected (+Q) results in parentheses. [d] MRCI(0.02)/[6s5p2d1f/5s4p2d1f] based on a larger CASSCF than in *c*; +Q results in parentheses. Dipole moments (μ) of $X^3\Pi$ and $A^3\Sigma^-$ states 2.590 and 1.652 D, respectively. [e] DFT-GGA(LSDA)/6-311G**. [f] CCSD(T)/[7s7p5d4f/7s7p4d3f]; $\mu(^3\Pi) = 2.636$ D, $\mu(^3\Sigma^-) = 1.606$ D. [g] DFT-B3LYP/6-311+G* (B3LYP/cc-pVDZ). [h] DFT-GGA/DNP; $\mu = 3.06$ D. [i] DFT-GGA/[6s5p4d/5s4p4d]. [j] DFT-BP86/6-31G(d). [k] MRDCI/[7s5p3d1f/5s4p3d1f] molecular orbitals (natural orbitals) based on HF orbitals of the $A^3\Sigma^-$ state; $\mu(X^3\Pi) = 2.62$ D, $\mu(A^3\Sigma^-) = 1.16$ D. [l] DFT-B3LYP/6−31G(d). [m] The energy and internuclear distance are calculated at the CCSD(T)/aug-cc-pVQZ level of theory, the ω_e at the CCSD(T)/ aug-cc-pV(Q+d)Z, whereas the dissociation energy is obtained after CBS(DTQ) extrapolation and corrected for core−valence, scalar relativistic, and spin−orbit effects. [n] FCI/cc-pVTZ. [o] Emission spectroscopy [p] Laser fluorescence spectroscopy, in conjunction with data from ref 1 for the $X^3\Pi$ state. [q] Knudsen cell mass spectroscopy.

TABLE 2: Total Energies (E_h) of the Al $^2P(3s^23p^1)$, $^2S^*(3s^24s^1)$, $^4P(3s^13p^2)$, $^2D(3s^23d^1)$, and $^2P^*(3s^24p^1)$ and the N $^4S(2s^22p^3)$, $^2D(2s^22p^3)$, and $^2P(2s^22p^3)$ Terms along with Their Corresponding Energy Splittings (eV) at the MRCI Level of Theory[a]

Al				
$^2P(3s^23p^1)$	$^2S^*(3s^24s^1)$	$^4P(3s^13p^2)$	$^2D(3s^23d^1)$	$^2P^*(3s^24p^1)$
−241.934 424	−241.818 379	−241.807 579	−241.787 114	−241.784 466
$^2S^* \leftarrow {}^2P$	$^4P \leftarrow {}^2P$	$^2D \leftarrow {}^2P$	$^2P^* \leftarrow {}^2P$	
3.158(3.133)	3.452(3.598)	4.009(4.012)	4.081(4.077)	

N		
$^4S(2s^22p^3)$	$^2D(2s^22p^3)$	$^2P(2s^22p^3)$
−54.523 306	−54.434 272	−54.391 431
$^2D \leftarrow {}^4S$	$^2P \leftarrow {}^4S$	
2.423(2.384)	3.589(3.576)	

[a] Experimental results in parentheses. Ref 20.

2. Methods

The correlation consistent basis sets aug-cc-pV5Z for Al and cc-pV5Z for N, generally contracted to [8s7p5d4f3g2h/$_{Al}$-6s5p4d3f2g1h/$_N$] ≡ A5Z were used through all our calculations.[15] The weighted core-valence cc-pwCV5Z basis set for Al contracted to [11s10p8d6f4g2h] ≡ C5Z[16] was also employed for the two lowest states $^3\Pi$ and $^3\Sigma^-$.

Our aim to construct PECs as well as the intense multireference character of the AlN system (see below) makes the use of a multi-reference method mandatory. Therefore, the CASSCF method was used to construct the reference space; additional "hard" (dynamic) correlation was obtained through single and double excitations (CASSCF+1+2 = MRCI) out of the CAS. With the exception of three Rydberg states, the zeroth-order spaces were formed by allotting the eight valence electrons (3 on Al + 5 on N) to the conventional valence orbital space (3s+3p on Al and 2s+2p on N), ranging from 400 to 600 configuration functions (CF). The corresponding MRCI spaces range from 14 × 10^6 to 25 × 10^6 CFs, reduced by an order of magnitude by applying the internally contracted (ic) approximation as implemented in the MOLPRO suite of codes.[17]

The calculation of Rydberg states requires the extension of the reference space by including the 4s and 4p Rydberg atomic orbitals of Al. For technical reasons, we were also forced to include in the active space the $3d_{z^2}$, $3d_{xz}$, and $3d_{yz}$ functions for the $^3A_2$ states, whereas the $3d_{z^2}$ and $3d_{x^2-y^2}$ orbitals were deemed as necessary for the $^5A_2$ states. The ensuing MRCI spaces however were too large, thus the N 2s orbital was excluded from the active space. The resulting zeroth-order function gives rise to MRCI spaces ranging from 370 × 10^6 ($^3A_2$) to 430 × 10^6 ($^5A_2$) CFs reduced by a factor of about 20 at the icMRCI level.

For only the two lowest states ($^3\Pi$ and $^3\Sigma^-$), core-valence (C-MRCI) and valence scalar relativistic effects were taken into account; the latter through the second-order Douglas−Kroll−Hess (DKH2) approximation.[18]

Basis set superposition error (BSSE)[19] corrections for the $^3\Pi$ and $^3\Sigma^-$ states at the MRCI, C-MRCI, and MRCI+DKH2 level are as follows (in kcal/mol): $^3\Pi$ 0.153, 0.646, and 0.133; $^3\Sigma^-$ 0.123, 0.718, and 0.124, respectively.

3. Atoms

The molecular states studied in the present work correlate to Al $^2P(3s^23p^1)$, $^2S^*(3s^24s^1)$, $^4P(3s^13p^2)$, $^2D[\simeq(0.73)3s^23d^1 + (0.21)3s^13p^2]$, $^2P^*(3s^24p^1)$, and N $^4S(2s^22p^3)$, $^2D(2s^22p^3)$, $^2P(2s^2-2p^3)$ atomic states. Note that the $^2S^*$ and $^2P^*$ terms of Al are of Rydberg character.[20] Table 2 lists their energy separations obtained at the MRCI/A5Z level of theory. With the exception of the ΔE(Al)($^4P \rightarrow {}^2P$) splitting, which differs by less than 1200 cm^{-1} from the experimental value, the rest of the numbers are in excellent agreement with the experiment.[20]

4. Results and Discussion

We have constructed 45 PECs of AlN spanning an energy range of 7.0 eV. In particular, the following states have been examined in ascending energy order of their asymptotes:

$$Al(^2P) + N(^4S) \rightarrow AlN[^{3,5}(\Sigma^-, \Pi)]$$

$$Al(^2P) + N(^2D) \rightarrow AlN[^{1,3}(\Sigma^+, \Sigma^-(2), \Pi(3), \Delta(2), \Phi)]$$

$$Al(^2S^*) + N(^4S) \rightarrow AlN(^{3,5}\Sigma^-)$$

$$Al(^2P) + N(^2P) \rightarrow AlN[^{1,3}(\Sigma^+(2), \Sigma^-, \Pi(2), \Delta)]$$

$$Al(^4P) + N(^4S) \rightarrow AlN[^{1,3}(\Sigma^+, \Pi)]$$

$$Al(^2D) + N(^4S) \rightarrow AlN(^3\Delta, {}^5\Delta, {}^5\Sigma^-)$$

$$Al(^2P^*) + N(^4S) \rightarrow AlN(^5\Sigma^-)$$

All states have been calculated from the first four channels (4, 18, 2, and 12), 4 out of 8 from the fifth, 3 out of 6 from the sixth, and 1 out of 4 from the seventh ($^5\Sigma^-$); one more state of $^5\Sigma^-$ symmetry has been examined, but we are not certain of its end products. Figure 1 shows the MRCI/A5Z PECs of all 45 states, Figure 2 shows a level diagram of 41 bound or with local minima states, and Figures 3−9 show PECs more or less according to their symmetry. In what follows, we discuss our results grouping the states in accordance with their origin. Tables 3 and 4 present results for all AlN bound states studied.

A. States $X^3\Pi$, $A^3\Sigma^-$, $9^5\Pi$, and $^5\Sigma^-$(repulsive). From the present work, it seems that the lowest $^3\Pi$ state is the ground state of AlN, *formally* tagged as $X^3\Pi$. The bonding can be described by the following valence−bond−Lewis (vbL) diagram, supported by the leading CASSCF equilibrium configuration, $|X^3\Pi\rangle \simeq 0.95|1\sigma^22\sigma^23\sigma^11\pi_x^11\pi_y^2\rangle$ (counting valence orbitals only), and the Mulliken atomic densities (Al/N) $3s^{1.59}$-$3p_z^{0.40}3p_x^{0.13}3p_y^{0.38}(3d)^{0.16}/2s^{1.82}2p_z^{1.11}2p_x^{0.84}2p_y^{1.52}$.

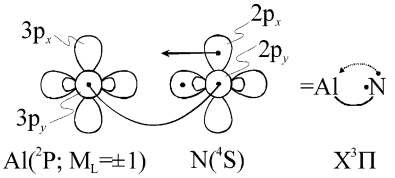

The N atom appears negatively charged by about 0.3 e$^-$, the result of Al−to−N π charge transfer. The attractive interaction

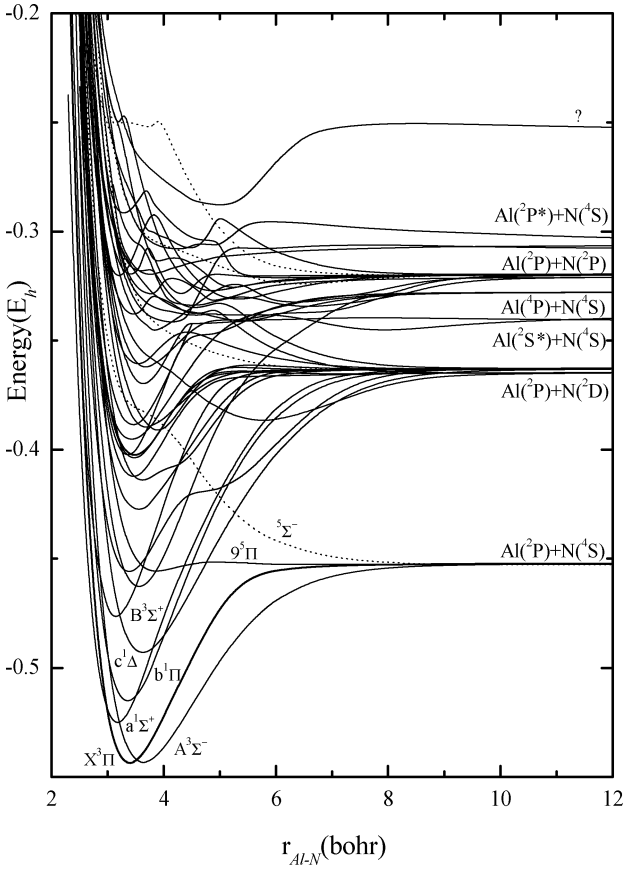

Figure 1. MRCI/A5Z PECs of 45 AlN states. All energies are shifted by +296.0 E_h.

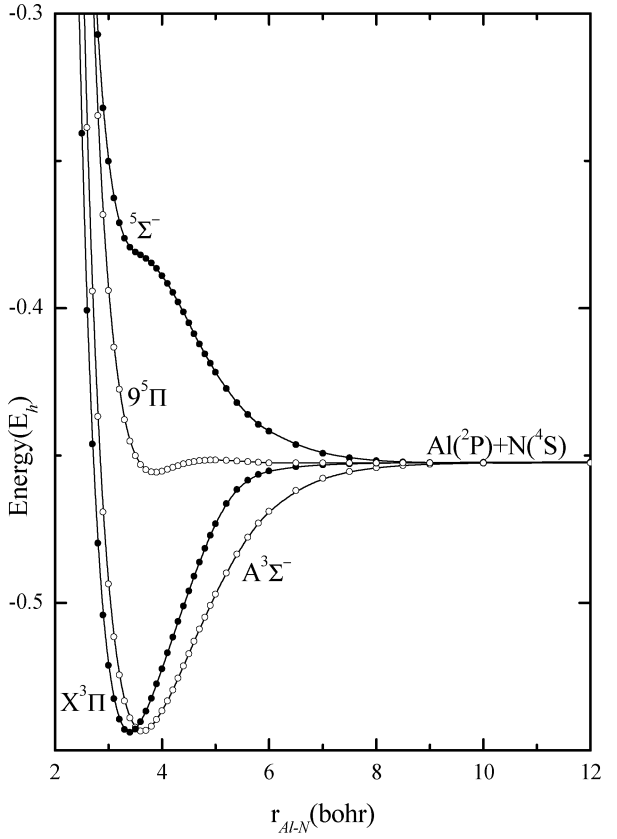

Figure 3. All MRCI/A5Z PECs stemming from the ground state atoms, Al(^{2}P) + N(^{4}S). All energies are shifted by +296.0 E_h.

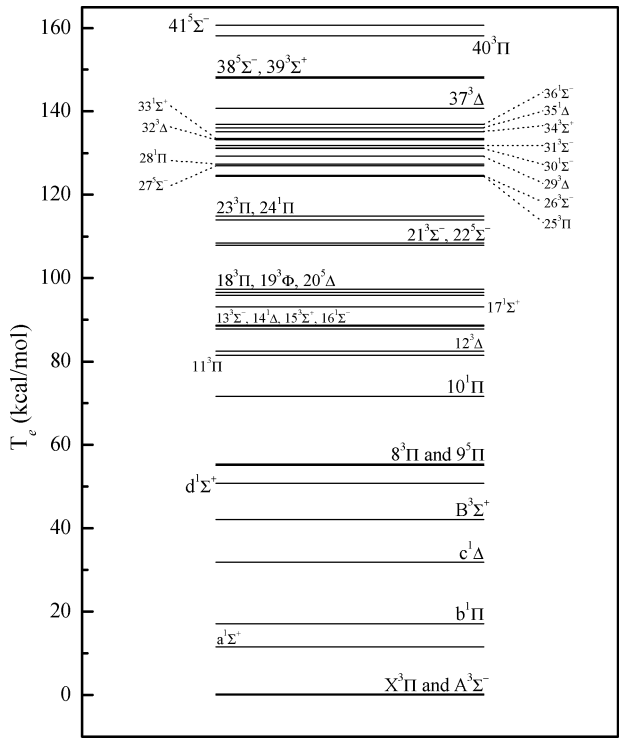

Figure 2. MRCI/A5Z relative energies of 36 bound states and 5 unbound states ($24^1\Pi$, $29^3\Delta$, $30^1\Sigma^-$, $39^3\Sigma^+$, $40^3\Pi$) featuring local minima of AlN.

can be ascribed to a complete and a partial π bonds as depicted in the diagram above; no σ interaction is observed. The MRCI(+Q)/A5Z bond distance and dissociation energy are r_e = 1.795(1.798) Å and D_e = 57.57(58.5) kcal/mol, or D_e = 57.15(58.1) kcal/mol taking into account the BSSE (−0.15 kcal/mol) and DKH2 (−0.27 kcal/mol) corrections (Table 3). Including the zero point energy effect (ZPE), D_0 = 56.27(57.0) kcal/mol. At the C-MRCI(+Q)/C5Z level r_e = 1.783(1.787) Å and D_e = 57.39(58.6) kcal/mol. The latter value becomes 56.47-(57.7) kcal/mol upon correcting for BSSE (0.65 kcal/mol) and the valence DKH2. Finally, $D_0 = D_e$ − ZPE = 55.37(56.6) kcal/mol.

From the analysis above, the recommended dissociation energy is $D_0 = 56.0 \pm 0.5$ kcal/mol at $r_e = 1.783$ Å. We remind that the corresponding experimental values are $D = 66 \pm 9$ kcal/mol[11] and $r_e = 1.7864$ Å,[1] whereas the recent coupled-cluster results of Grant and Dixon[7] are similar to ours: D_0 = 57.01 kcal/mol and $r_e = 1.803$ Å for the $^3\Pi$ state but predicted to be 155 cm^{-1} above the $^3\Sigma^-$ state.

The next state of $^3\Sigma^-$ symmetry can be considered as degenerate to the $X^3\Pi$ state, formally characterized as $A^3\Sigma^-$. Its leading CASSCF configuration, $0.96\ |1\sigma^2 2\sigma^2 3\sigma^2 1\pi_x^1 1\pi_y^1\rangle$, and Mulliken atomic populations, $3s^{1.76}3p_z^{0.53}3p_x^{0.12}3p_y^{0.12}$-$(3d)^{0.13}/2s^{1.85}2p_z^{1.62}2p_x^{0.92}2p_y^{0.92}$ point to the following bonding vbL diagram:

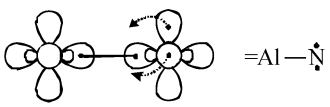

Similarly to the X $^3\Pi$ state, about 0.3 e$^-$ are transferred from Al to N; in detail, 0.5 e$^-$ migrate to the $2p_z$ orbital of N resulting to the σ bond, while 0.2 e$^-$ are moving back through the p_π system contributing slightly to the bonding. The MRCI(+Q)/

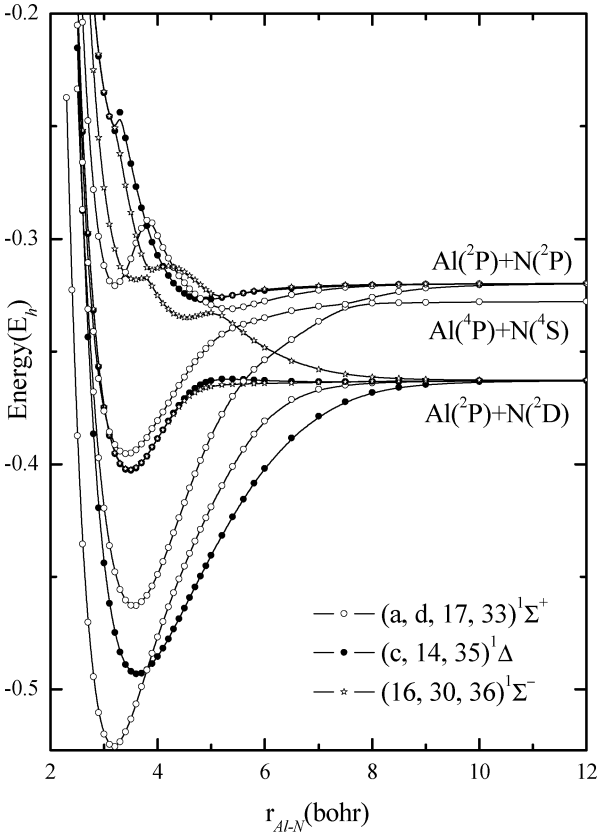

Figure 4. Ten MRCI/A5Z PECs of $^1A_1(^1\Sigma^+)$ and $^1A_2(^1\Sigma^-,^1\Delta)$ symmetry. All energies are shifted by +296.0 E_h.

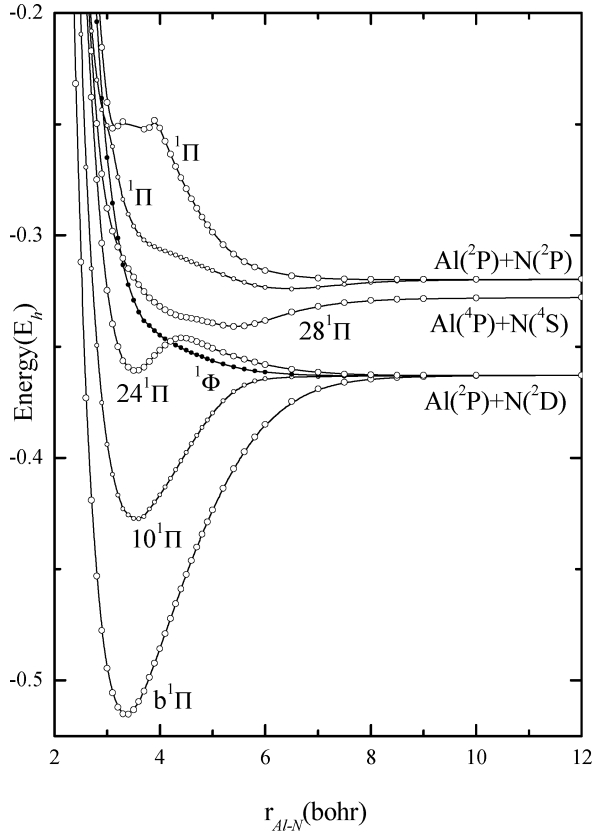

Figure 5. Seven MRCI/A5Z PECs of $^1B_1(^1\Pi, ^1\Phi)$ symmetry. All energies are shifted by +296.0 E_h.

A5Z and C-MRCI(+Q)/C5Z r_e and D_e values are 1.922(1.926) Å and 57.42(57.7) kcal/mol and 1.909(1.913) Å and 57.67(58.6) kcal/mol, respectively (Table 3). Correcting as before for relativity and BSSE, we obtain D_e = 57.09(57.3) and 56.74-(57.6) kcal/mol for the "valence" and "core" results, respectively. Based on the final D_e values of the $X^3\Pi$ and $A^3\Sigma^-$ states, "valence" and "core" $T_e(A^3\Sigma^- \leftarrow X^3\Pi)$ separations are 21(280) and −94(35) cm^{-1}.

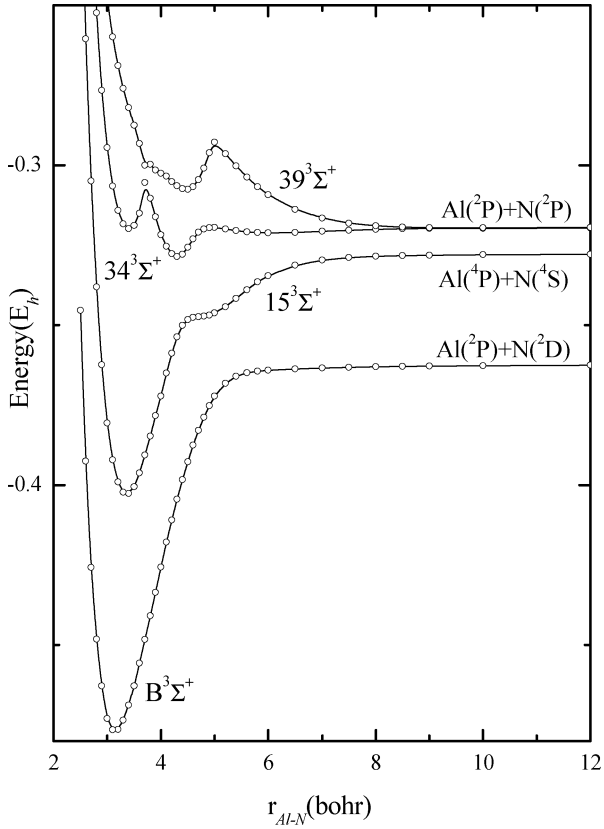

Figure 6. MRCI/A5Z PECs of (B, 15, 34, 39)$^3\Sigma^+$ States. All energies are shifted by +296.0 E_h.

The corresponding D_0 values for the $A^3\Sigma^-$ state are 56.19-(56.4) and 55.83(56.7) kcal/mol with T_0 = 28(210) and 224-(350) cm^{-1}. Obviously, the $X^3\Pi$ and $A^3\Sigma^-$ states are strictly degenerate within the accuracy of our computations, rendering the symbols "X" and "A" only formal. An experimental definitive verdict of the $X^3\Pi$ and $A^3\Sigma^-$ ordering would be certainly interesting; however, this can be a difficult task considering the geometry of their PECs (Figure 3).

It is perhaps of interest at this point to contrast our findings for these two states with the results of the isovalent molecules BN, GaN, and InN. For the GaN and InN the manifold of states within 3 eV is strikingly similar to those of AlN. In particular, the two lowest states of GaN ($X^3\Sigma^-$, $A^3\Pi$)[21] and InN($X^3\Sigma^-$, $A^3\Pi$)[22] are practically degenerate with T_e values of 532 and 323 cm^{-1} and D_e values of 46.5 and 42.4 kcal/mol, respectively, both correlating to the ground-state fragments. In addition, the second excited state of GaN and InN of similar symmetry to AlN, $a^1\Sigma^+$, lie 17.5[21] and 19.4[22] kcal/mol above the $X^3\Sigma^-$ state, as compared to 11.5 kcal/mol for AlN (*vide infra*), correlating adiabatically to ^{2}P(Ga, In, Al) + ^{2}D(N). However, the *in situ* metals M(Al, Ga, In) in the $a^1\Sigma^+$ state find themselves in the $^4P(ns^1np^2; n = 3, 4, 5)$ state of the M atom, the result of a strong interaction with another $^1\Sigma^+$ state ($d^1\Sigma^+$ for AlN) correlating to M(^{4}P) + N(^{4}S).

The situation for the BN molecule is somewhat different. Two states are also competing for the ground state but now with

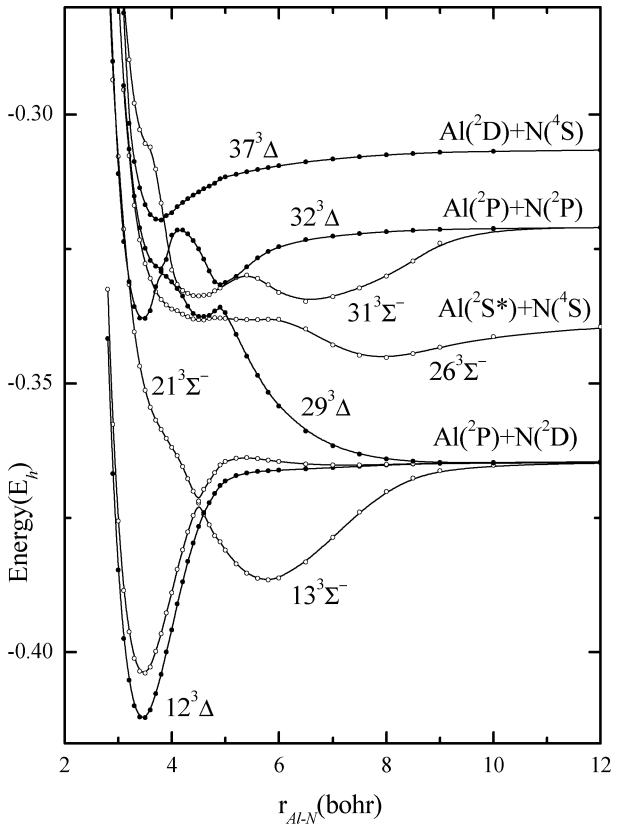

Figure 7. Eight MRCI/A5Z PECs of $^3A_2(^3\Sigma^-,^3\Delta)$ symmetry. All energies are shifted by +296.0 E_h.

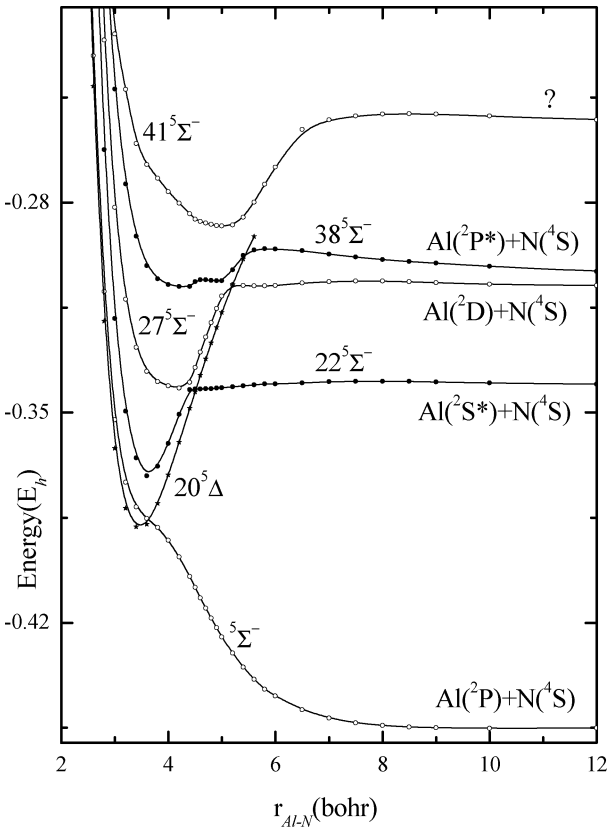

Figure 9. MRCI/A5Z PECs of all $^5\Sigma^-$ states considered and of one $^5\Delta$. All energies are shifted by +296.0 E_h.

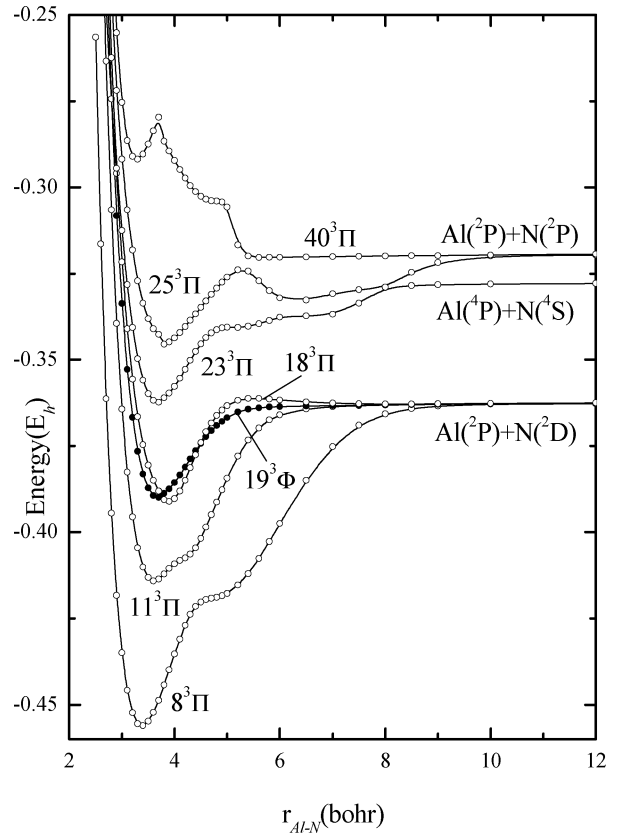

Figure 8. Seven MRCI/A5Z PECs of $^3B_1(^3\Pi, ^3\Phi)$ symmetry. All energies are shifted by +296.0 E_h.

symmetries $X^3\Pi$ and $a^1\Sigma^+$, the energy difference being 95 cm^{-1}, whereas the $B^3\Sigma^-$ is located 28.4 kcal/mol higher at the MRCI/4Z level of theory.[13] In addition, the binding energies of the $X^3\Pi$ and $B^3\Sigma^-$ states for BN with respect to the ground-state atoms are D_e = 102.2 and 73.7 kcal/mol, respectively;[13] the binding energy of $a^1\Sigma^+$ is 158.8 kcal/mol with respect to B(^{2}P) + N(^{2}D). The corresponding D_e values of the $^1\Sigma^+$ state for AlN, GaN,[21] and InN[22] are 102.1, 86 (as deduced from Figure 1 of ref 21), and 82.8 kcal/mol, respectively. These differences between BN and MN (M = Al, Ga, In) are rather a "size effect" as is evident from the atomic radii of (in Å) B(0.79), Al(1.43), Ga(1.22), and In(1.63)[23] and reflected to the r_e values (X states for instance) of BN(1.330),[13] AlN(1.783), GaN(1.964),[21] and InN(2.140).[22]

The $9^5\Pi$ state, as expected, is of single reference character (i.e., $|9^5\Pi\rangle \simeq 0.97|1\sigma^2 2\sigma^2 3\sigma^1 1\pi_x^1 1\pi_y^1 2\pi_y^1\rangle$) with a shallow minimum of about 2.5 kcal/mol at r_e = 2.05 Å (Figure 3, Table 4). The $^5\Sigma^-$ state with the symmetry carrying electron of Al along the internuclear axis (M_L = 0) is purely repulsive (Figure 3).

B. States [$a^1\Sigma^+$, (16, 30)$^1\Sigma^-$, (b, 10, 24)$^1\Pi$, (c, 14)$^1\Delta$, $^1\Phi$-(repulsive)] and [$B^3\Sigma^+$, (13, 21)$^3\Sigma^-$, (8, 11, 18)$^3\Pi$, (12, 29)$^3\Delta$, 19$^3\Phi$]. The channel Al(^{2}P) + N(^{2}D) gives rise to the above 18-state manifold (9 singlets and 9 triplets), 14 of which are strongly bound. Their MRCI/A5Z relative ordering and PECs are shown in Figures 2 and 4−8; numerical results are listed in Tables 3 and 4. With the exception of the $c^1\Delta$ state, the rest are of intense multireference character. In what follows the most interesting of the states will be discussed briefly in ascending energy order.

$a^1\Sigma^+$. This is the second excited-state located 11.53 kcal/mol above the X state. At the MRCI(+Q)/A5Z we obtain r_e = 1.682(1.675) Å and D_e = 102.12(103.5) kcal/mol with respect to the adiabatic products or 46.04(48.9) kcal/mol with respect to the ground-state atoms, as contrasted to the experimental values of 1.65 Å and 87.22 kcal/mol.[12] In the light of these

TABLE 3: Total Energies E (E_h), Bond Distances r_e (Å), Dissociation Energies D_e (kcal/mol), Dipole Moments μ (D), Harmonic Frequencies ω_e (cm^{-1}), Anharmonic Corrections $\omega_e x_e$(cm^{-1}), Rotational−Vibrational Constants α_e (cm^{-1}), Zero Point Energies ZPE (cm^{-1}), and Separation Energies T_e (kcal/mol) of the $X^3\Pi$, $A^3\Sigma^-$, $a^1\Sigma^+$, $b^1\Pi$, $c^1\Delta$, $B^3\Sigma^+$, and $d^1\Sigma^+$ States of AlN

state	method	$-E$	r_e	D_e[a]	$<\mu>/\mu_{ff}$[b]	ω_e	$\omega_e x_e$	α_e	ZPE	T_e
$X^3\Pi$	CASSCF	296.370 34	1.807	45.05		732.9	4.45	0.0004	369	0
	MRCI	296.543 877	1.795	57.57	2.74/2.72	757.5	5.50	0.0057	378	0
	MRCI+Q	296.556 1	1.798	58.5		751.6	5.52	0.0057	375	0
	C-MRCI	296.838 555	1.783	57.39	2.60/2.77	770.8	5.52	0.0057	384	0
	C-MRCI+Q	296.868 9	1.787	58.6		763.8	5.49	0.0057	381	0
	CASSCF	296.835 46	1.807	44.94		738.2	4.73	0.0060	368	0
	MRCI+DKH2	297.008 862	1.794	57.30	2.71/2.70	757.4	5.51	0.0058	377	0
	MRCI+DKH2+Q	297.021 1	1.797	58.2		751.0	5.47	0.0057	374	0
	expt.		1.7864[c]	66 ± 9[d]		758.4[c]	5.7[c]			
$A^3\Sigma^-$	CASSCF	296.372 20	1.930	43.96		618.1	4.52	0.0052	308	−1.17
	MRCI	296.543 553	1.922	57.42	1.57/1.56	629.5	4.59	0.0051	314	0.20
	MRCI+Q	296.554 2	1.926	57.7		623.9	4.69	0.0052	311	1.23
	C-MRCI	296.839 335	1.909	57.67	1.51/1.57	639.6	4.45	0.0051	319	−0.49
	C-MRCI+Q	296.868 1	1.913	58.6		633.3	4.38	0.0051	316	0.50
	CASSCF	296.836 74	1.978	43.41		786.9	26.49	0.0057	260	−0.80
	MRCI+DKH2	297.008 663	1.923	57.21	1.51/1.56	688.6	21.06	0.0031	351	0.12
	MRCI+DKH2+Q	297.019 2	1.925	57.4		629.5	6.64	0.0052	314	1.18
$a^1\Sigma^+$	CASSCF	296.327 29	1.721	85.45					511	27.01
	MRCI	296.525 498	1.682	102.12	4.54/4.47	965.2	12.14	0.0031	480	11.53
	MRCI+Q	296.540 9	1.675	103.5					472	9.54
	expt.[e]		1.65	87.22		930	6.5			
$b^1\Pi$	CASSCF	296.342 39	1.771	90.40					419	17.54
	MRCI	296.516 563	1.764	96.10	4.04/3.92	835.6	7.00	0.0047	418	17.14
	MRCI+Q	296.528 6	1.767	96.3					416	17.27
$c^1\Delta$	CASSCF	296.291 92	1.919	63.25					303	49.21
	MRCI	296.493 219	1.920	81.87	1.41/1.38	640.0	1.45	0.0016	317	31.79
	MRCI+Q	296.509 2	1.933	83.5					315	29.47
$b^3\Sigma^+$	CASSCF	296.285 25	1.717	59.26					441	53.40
	MRCI	296.476 799	1.666	71.75	4.07/3.95	947.8	−1.83	0.0060	467	42.09
	MRCI+Q	296.493 1	1.656	73.7					486	39.57
$d^1\Sigma^+$	CASSCF	296.268 07	1.907	122.28					335	64.17
	MRCI	296.462 946	1.883	84.87	1.32	732.2	4.01	0.0027	366	50.79
	MRCI+Q	296.477 9	1.886	89.2					360	49.07

[a] With respect to the adiabatic products. [b] The dipole moments have been calculated as expectation values ($<\mu>$) and with the finite field approach (μ_{ff}). Field strengths range from 10^{-6} to 10^{-4} au. [c] Ref 2. [d] Ref 11. [e] Ref 12.

numbers, we believe that the experimental dissociation energy is certainly in error.

The $a^1\Sigma^+$ dissociates to

$$|^2P; M_L = \pm 1\rangle_{Al} \times |^2D; M_L = \mp 1\rangle_N = 0.49|2s^2 3s^2 2p_z^2 (2p_x^1 3\bar{p}_x^1 + 2p_y^1 3\bar{p}_y^1)\rangle - 0.49|2s^2 3s^2 (2p_x^2 2p_y^1 3\bar{p}_y^1 + 2p_x^1 3\bar{p}_x^1 2p_y^2)\rangle$$

The CASSCF equilibrium CFs and Mulliken densities are

$$|a^1\Sigma^+\rangle \simeq 0.73|1\sigma^2 2\sigma^2 1\pi_x^2 1\pi_y^2\rangle + 0.38|1\sigma^2 2\sigma^1 3\bar{\sigma}^1 1\pi_x^2 1\pi_y^2\rangle - 0.17|1\sigma^2 3\sigma^2 1\pi_x^2 1\pi_y^2\rangle + 0.26|1\sigma^2 2\sigma^2 (1\pi_x^2 1\pi_y^1 2\bar{\pi}_y^1 + 1\pi_x^1 2\bar{\pi}_x^1 1\pi_y^2)\rangle$$

$$3s^{1.14} 3p_z^{0.24} 3p_x^{0.52} 3p_y^{0.52} (3d)^{0.14} / 2s^{1.76} 2p_z^{0.79} 2p_x^{1.41} 2p_y^{1.41}$$

indicating the excited $^4P(3s^1 3p^2)$ *in situ* character of the Al atom due to the interaction of the $a^1\Sigma^+$ and $d^1\Sigma^+$ states (Figure 4). The emerging bonding picture can be represented graphically by the following vbL diagram:

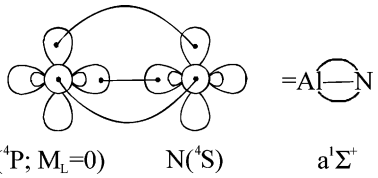

A total of 0.4 e^- are moving from Al to N, perhaps the cause of a large dipole moment $\mu = 4.5$ D, the largest of all states studied.

$b^1\Pi$. This is the third excited state having a $T_e = 17.14$ kcal/mol and correlating to $|^2P; M_L = \pm 1\rangle_{Al} \times |^2D; M_L = 0\rangle_N$. The main CASSCF equilibrium CFs $|b^1\Pi\rangle \simeq |1\sigma^2 2\sigma^2 3\sigma^1 1\bar{\pi}_x^1 - [(0.86)1\pi_y^2 + (0.32)1\pi_y^1 2\bar{\pi}_y^1]\rangle$ along with the atomic Mulliken populations $3s^{1.31} 3p_z^{0.45} 3p_x^{0.14} 3p_y^{0.63} (3d)^{0.13} / 2s^{1.86} 2p_z^{1.27} 2p_x^{0.85} - 2p_y^{1.32}$, support the following bonding picture:

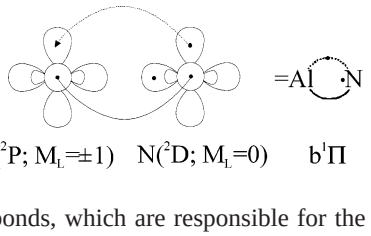

The 1+1/2 π bonds, which are responsible for the stability of AlN in this state, engender a $D_e = 96.10(96.3)$ kcal/mol and $r_e = 1.764(1.767)$ Å at the MRCI(+Q) level. A total Mulliken charge transfer of 0.3 e^- from Al to N is observed.

The next state, $c^1\Delta$ has a T_e value of 31.79 kcal/mol, $D_e = 81.87$ kcal/mol at $r_e = 1.920$ Å, and correlates to $|^2P; M_L = \pm 1\rangle_{Al} \times |^2D; M_L = \pm 1\rangle_N$. The asymptotic configurations are identical to those of the $a^1\Sigma^+$ state (with a sign flip), whereas at the equilibrium, after an interaction with the $14^1\Delta$ near 10 bohr (Figure 4), the molecule is fully described by two configurations: $|c^1\Delta\rangle \simeq 0.68|1\sigma^2 2\sigma^2 3\sigma^2 -$

TABLE 4: Total Energies E (E_h), Bond Distances r_e (Å), Dissociation Energies D_e (kcal/mol), Dipole Moments μ (D), Harmonic Frequencies ω_e (cm^{-1}), Anharmonic Corrections $\omega_e x_e$ (cm^{-1}), Rotational−Vibrational Constants α_e (cm^{-1}), Zero Point Energies ZPE (cm^{-1}), and Separation Energies T_e (kcal/mol) of the Last 34 States of AlN at the MRCI Level of Theory[a]

state[b]	$-E$	r_e	D_e[c]	μ[d]	ω_e	$\omega_e x_e$	α_e	ZPE	T_e
$8^3\Pi$	296.456 149	1.787	58.76	2.10	754.8	7.13	0.0071	376	55.05
	(296.470 0)	(1.782)	(59.3)					(376)	(54.0)
expt.[e]		1.7672			779.4	11.0			56.40
$9^5\Pi$	296.455 658	2.045	2.0	0.69	328.8		0.0212	181	55.36
	(296.467 6)	(2.057)	(2.5)					(178)	(55.6)
$10^1\Pi$	296.429 750	1.883	42.06	1.64				337	71.62
	(296.442 9)	(1.889)	(42.0)						(71.1)
$11^3\Pi$	296.414 104	1.913	32.30	1.56	699.6		0.0026	311	81.43
	(296.428 9)	(1.920)	(33.4)						(79.9)
$12^3\Delta$	296.412 423	1.821	30.28	2.32	714.4	1.27	0.0013	357	82.49
	(296.427 8)	(1.836)	(32.6)					(342)	(80.5)
$13^3\Sigma_G^-$	296.404 003	1.833	24.96	2.24	709.1	3.13	−0.0013	345	87.77
	(296.420 1)	(1.951)	(28.0)					(339)	(85.4)
$13^3\Sigma_L^-$	296.386 583	3.060		1.95	214.0	1.36	0.0004	106	
	(296.400 2)	(3.107)						(109)	
$14^1\Delta_G$	296.402 842	1.837	25.18	2.34	682.8	8.06	0.0050	337	88.50
	(296.422 1)	(1.843)	(29.0)					(341)	(84.1)
$14^1\Delta_L$	296.363 352	3.754						18	
	(296.376 9)	(3.509)						(19)	
$15^3\Sigma^+$	296.402 788	1.779	47.10	2.89	864.0	0.32	0.0012	431	88.53
	(296.421 3)	(1.781)	(53.7)					(423)	(84.6)
$16^1\Sigma^-$	296.402 580	1.838	25.03	2.32	674.5	7.31	0.0065	336	88.67
	(296.421 1)	(1.842)	(28.4)					(339)	(84.7)
$17^1\Sigma^+$	296.395 425	1.812	47.53	2.20	625.6	2.78	0.0022	313	93.16
	(296.413 7)	(1.814)	(51.3)					(310)	(89.4)
$18^3\Pi$	296.391 137	2.054	18.05	0.47	677.0	15.2	0.0020	326	95.85
	(296.408 7)	(2.047)	(20.6)					(306)	(92.5)
$19^3\Phi$	296.389 961	1.948	17.23	1.33	638.8	28.7	0.0190	338	96.58
	(296.404 38)	(1.9658)	(18.1)					(286)	(95.3)
$20^5\Delta$	296.388 743	1.833	51.56	1.11	716.9	2.13	−0.0021	358	97.35
	(296.401 7)	(1.797)	(53.7)						(96.9)
$21^3\Sigma^-$	296.371 923	2.379	5.19	2.01				482	107.90
	(296.388 7)	(2.38)	(8.1)						(105)
$22^5\Sigma^-$	296.371 155	1.916	19.19		923.3	−2.99	0.017	465	108.4
	(296.383 6)	(1.911)	(23.4)					(423)	(108)
$23^3\Pi$	296.362 341	1.946	21.69	1.35	650.8	12.0	0.023	347	113.9
	(296.378 7)	(2.002)	(27.0)					(284)	(111)
$24^1\Pi$	296.360 900	1.872		1.92	648.8	10.5	−0.0036	323	114.8
	(296.388 6)	(1.848)	(8.0)					(612)	(105)
$25^3\Pi$	296.345 547	2.018	16.31		657.0	41.0	0.020	346	124.4
$26^3\Sigma^-$	296.345 255	4.181	4.41	3.55				60	124.6
	(296.356 6)	(4.143)	(6.2)					(68)	(125)
$27^5\Sigma^-$	296.341 610	2.194	21.20	2.93	496.9	3.60	0.0036	225	126.9
	(296.352 5)	(2.308)	(23.8)					(619)	(127.76)
$28^1\Pi$	296.340 957	2.871	8.26		241.3	9.23	−0.010	116	127.3
$29^3\Delta_G$	296.337 97	1.852		1.58					129.2
$29^3\Delta_L$	296.337 629	2.399		1.43				224	
$30^1\Sigma_G^-$	296.334 937	2.408		1.12				184	131.1
	(296.351 6)	(2.396)							(128)
$30^1\Sigma_L^-$	296.318 086	1.896							
$31^3\Sigma_G^-$	296.334 805	3.46	8.66	3.87				87	131.2
$31^3\Sigma_L^-$	296.333 799	2.367	8.03	0.65				124	131.8
$32^3\Delta_G$	296.331 666	2.587	6.69	0.13	401.8	15.2	0.0144	227	133.2
$32^3\Delta_L$	296.328 781	2.006		0.99					
$33^1\Sigma_G^+$	296.331 188	2.819	7.23	0.99	297.5	11.5	0.0020	143	133.5
	(296.348 9)	(2.809)	(10.7)					(163)	(130)
$33^1\Sigma_L^+$	296.320 771	1.692		3.59	1039.8	11.8	0.0070	527	
	(296.337 5)	(1.698)							
$34^3\Sigma_G^+$	296.328 623	2.279	5.68	1.13	345.96			346	135.1
	(296.343 8)	(2.290)	(7.7)					(336)	(133)
$34^3\Sigma_L^+$	296.321 150	3.224		1.03				38	
	(296.333 7)	(3.176)						(38)	
$34^3\Sigma_{vdW}^+$[f]	296.319 847	1.803							
	(296.339 5)	(1.785)							
$35^1\Delta$	296.327 064	2.576	4.63	0.38				139	136.0
	(296.343 5)	(2.542)	(7.3)					(167)	(133)
$36^1\Sigma^-$	296.325814	2.757	3.92	0.13				185	136.8

TABLE 4: (Continued)

state[b]	$-E$	r_e	D_e[c]	μ[d]	ω_e	$\omega_e x_e$	α_e	ZPE	T_e
$37^3\Delta$	296.319 696	1.994	8.23	0.30	459.0	30.8	0.0122	235	140.7
	(296.332 5)	(1.982)	(10.3)					(257)	(140.30)
$38^5\Sigma^-$	296. 308 073	2.262	2.14						148.0
$39^3\Sigma^+$	296.307 605	2.369		0.31				261	148.3
	(296.322 8)	(2.370)						(224)	(146)
$40^3\Pi$	296.291 930	1.734			842.9	23.3	0.016	417.54	158.1
$41^5\Sigma^-$	296.287 900	2.681	21.93		251.1	−6.64	−0.016	138	160.6

[a] Results in parentheses after applying the Davidson correction (+Q). [b] Subscripts G and L refer to global and local minima, respectively. [c] With respect to the adiabatic products. [d] Dipole moments calculated as expectation values, $<\mu>$. [e] Ref 1. [f] van der Waals minimum.

$(1\pi_x^2 - 1\pi_y^2)\rangle$. In conjunction with the atomic equilibrium populations

$$3s^{1.77}3p_z^{0.48}3p_x^{0.14}3p_y^{0.14}(3d)^{0.14}/2s^{1.86}2p_z^{1.64}2p_x^{0.89}2p_y^{0.89}$$

the bonding is succinctly represented graphically as follows:

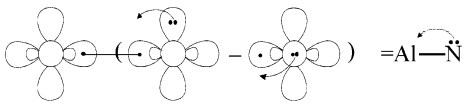

Approximately 0.5 e^- migrate from Al to N via the σ-frame, with 0.2 e^- returning back through the p_π system.

$B^3\Sigma^+$. The fifth excited state, 42.09 kcal/mol above $X^3\Pi$, is the complete analog of the $a^1\Sigma^+$ state but with the electrons of the σ bond coupled into a triplet (observe the scheme below). It correlates to $|^2P;\ M_L = \pm1\rangle_{Al} \times |\ ^2D;\ M_L = \mp1\rangle_N$ with asymptotic configurations identical to those of the $a^1\Sigma^+$ (of course the "bar" over the $3p_x$ and $3p_y$ orbitals is missing). At about 7 bohr interacts with the $15^3\Sigma^+$ which correlates to Al(^{4}P; $M_L = 0$) + N(^{4}S) (Figure 6), therefore acquiring this character close to equilibrium. The leading CASSCF configurations, analogous to those of the $a^1\Sigma^+$, and the corresponding atomic populations

$$|B^3\Sigma^+\rangle \simeq |1\sigma^2 2\sigma^1 3\sigma^1[(0.76)1\pi_x^2 1\pi_y^2 - (0.19)(1\bar{\pi}_x^1 2\pi_x^1 1\pi_y^2 + 1\pi_x^2 1\bar{\pi}_y^1 2\pi_y^1) + (0.24)(1\pi_x^1 2\bar{\pi}_x^1 1\pi_y^2 + 1\pi_x^2 1\pi_y^1 2\bar{\pi}_y^1)\rangle + 0.26|1\sigma^2 2\sigma^2(1\pi_x^2 1\pi_y^1 2\pi_y^1 + 1\pi_x^1 2\pi_x^1 1\pi_y^2)\rangle$$

$$3s^{0.91}3p_z^{0.46}3p_x^{0.49}3p_y^{0.49}(3d)^{0.21}/2s^{1.66}2p_z^{0.91}2p_x^{1.42}2p_y^{1.42}$$

suggest the following bonding scheme, comprising two pure π bonds and a partial σ bond.

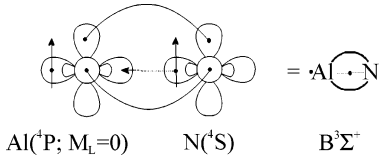

The transfer of 0.4 σ electrons from N to Al and 0.8 π electrons in reverse is the cause of the bonding and of a net Al−to−N electron transfer of about 0.4 e^-. The bond distance ($r_e = 1.666$ Å) and dipole moment ($\mu = 4.0$ D) are very similar to those of the $a^1\Sigma^+$ state. We touch now upon a few states that show some interesting features.

The $8^3\Pi$ is the only excited state where experimental parameters are available[2] and which compare favorably with the present calculated values (experimental results in parentheses): $r_e = 1.782$ (1.7672) Å, $\omega_e = 754.8$ (779.4) cm^{-1}, $\omega_e x_e = 7.13$ (11.0) cm^{-1}, $T_e = 55.05$ (56.40) kcal/mol.

The asymptotic CASSCF configurations of the $12^3\Delta$ and $29^3\Delta$ states are as follow:

$$|12^3\Delta\rangle = |\ ^2P;\ M_L = 0\rangle_{Al} \times |^2D;\ M_L = \pm2\rangle_N = 0.69|2s^2 3s^2 2p_z^1 3p_z^1(2p_x^2 - 2p_y^2)\rangle$$

$$|29^3\Delta\rangle = |^2P;\ M_L = \pm1\rangle_{Al} \times |^2D;\ M_L = \pm1\rangle_N = 0.49|2s^2 3s^2 2p_z^2(2p_x^1 3p_x^1 - 2p_y^1 3p_y^1)\rangle + 0.49|2s^2 3s^2(2p_x^2 2p_y^1 3p_y^1 - 2p_x^1 3p_x^1 2p_y^2)\rangle$$

At 8 bohr these two states exchange their M_L values, mirrored to the equilibrium CFs of the $12^3\Delta$ state:

$$|12^3\Delta\rangle \simeq 0.59|1\sigma^2 2\sigma^2(1\pi_x^1 2\pi x^1 1\pi_y^2 - 1\pi_x^2 1\pi_y^1 2\pi_y^1)\rangle$$

$$-0.22|1\sigma^2 3\sigma^2(1\pi_x^1 2\pi_x^1 1\pi_y^2 - 1\pi_x^2 1\pi_y^1 2\pi_y^1)\rangle$$

The $29^3\Delta$ state is of repulsive nature. However, an avoided crossing near 4.9 bohr with the $32^3\Delta$ (stemming from Al(^{2}P; $M_L = \pm1$) + N(^{2}P; $M_L = \pm1$)), and a second avoided crossing at 3.8 bohr again with the $32^3\Delta$ state, which already has suffered an avoided crossing with the $37^3\Delta$ state [correlating to Al(^{2}D; $M_L = \pm2$) + N(^{4}S)] at 4.2 bohr, result in two minima, a local (L) with $r_e^L = 2.40$ Å and a global (G) with $r_e^G = 1.85$ Å (see Figure 7). The barrier height measured from the G minimum is 5.6 kcal/mol. The CASSCF wavefunction of the $29^3\Delta_G$ state is indeed very complex, reflecting in part the complicated description of the Al ^{2}D term (see Section 3).

The PEC of the $13^3\Sigma^-$ state with end products Al(^{2}P; $M_L = 0$) + N(^{2}D; $M_L = 0$) displays an interesting morphology due to a severe avoided crossing with the $21^3\Sigma^-$ state [correlating to Al(^{2}P; $M_L = \pm1$) + N(^{2}D; $M_L = \mp1$)] at 4.5 bohr (Figure 7). The result is an exchange of the M_L values between the two states after the "crossing" point and the creation of two wells, a local ($r_e^L = 3.060$ Å) and a global ($r_e^G = 1.833$ Å). The dissociation energies with respect to the "L" and "G" minima are 14.0 and 25.0 kcal/mol. At 7.0 bohr the $21^3\Sigma^-$ state shows a van der Waals interaction of ~1 kcal/mol.

The $24^1\Pi$ state is unbound by 1.1 kcal/mol with respect to the end atoms, but it displays a minimum ($r_e = 1.872$ Å) due to an avoided crossing with the $28^1\Pi$ state which correlates to Al(^{4}P) + N(^{4}S). The barrier height measured from the minimum is 9.24 kcal/mol (Figure 5).

Finally, the $30^1\Sigma^-$ state being repulsive displays two shallow minima at distances 2.41 and 1.90 Å, the result of two avoided crossings with the $36^1\Sigma^-$ state. The latter correlates to Al(^{2}P; $M_L = \pm1$) + N(^{2}P; $M_L = \mp 1$) (Figure 4).

C. States $22^5\Sigma^-$ and $26^3\Sigma^-$. These are two states of extreme multi-reference description correlating to (Rydberg) Al(^{2}S*; $3s^2$-$4s^1$) + N(^{4}S). The $22^5\Sigma^-$, bound with respect to the adiabatic atoms by 19.2(23.5) kcal/mol at r_e = 1.916(1.911) Å, suffers an avoided crossing with the $27^5\Sigma^-$ near 4.4 bohr (Figure 9). The latter which correlates to Al(^{2}D) + N(^{4}S) has already experienced an avoided crossing close to 5.2 bohr with the $38^5\Sigma^-$ and with end products of Al(^{2}P*; $3s^24p^1$) + N(^{4}S). Therefore the *in situ* equilibrium atomic character of the $22^5\Sigma^-$ state is a mixture of Al(^{2}D) + Al(^{2}P*). The PEC of the $26^3\Sigma^-$ state has a rather "unconventional" shape featuring a shallow minimum of 4.4 kcal/mol at 8 bohr (Figure 7).

D. States $d^1\Sigma^+$, $15^3\Sigma^+$, $23^3\Pi$, $28^1\Pi$. Out of the eight states of symmetry^{1,3,5,7}(Σ^+, Π) emanating from the channel Al(^{4}P) + N(^{4}S), we have calculated the singlets and triplets. It should be noted at this point that experimentally[20] the asymptotic products Al(^{4}P) + N(^{4}S) are *higher* than the Al(^{2}P) + N(^{2}P) by 258 cm^{-1}; our calculations reverse the asymptotic ordering by 1785(881) cm^{-1} at the MRCI(+Q)/A5Z level. In ascending energy order these four states are 50.8, 88.5, 113.9, and 127.3 kcal/mol above the $X^3\Pi$ state, respectively.

Because of an avoided crossing between the $d^1\Sigma^+$ and the $17^1\Sigma^+$ states [the latter correlating to the channel Al(^{2}P) + N(^{2}P)] near 7.5 bohr, these two states exchange character. Thus the in *situ* equilibrium atoms of the $d^1\Sigma^+$ state correlate *diabatically* to Al(^{2}P; M_L = 0) + N(^{2}P; M_L = 0) (see Figure 4). With respect to the adiabatic atoms, D_e ($d^1\Sigma^+$) = 84.9(89) kcal/mol and r_e = 1.883(1.886) Å (Table 3).

The $15^3\Sigma^+$ interacts with the $B^3\Sigma^+$ state close to 7 bohr as discussed in Section 4B (Figure 6). According to Table 4, it is bound perhaps by more than 50 kcal/mol at r_e = 1.780 Å.

The $23^3\Pi$ state presents an irregular PEC as can be seen in Figure 8 due to interactions with the $25^3\Pi$ and higher (but not calculated) $^3\Pi$ states. It is bound by more than 20 kcal/mol at r_e = 1.946 Å.

The $28^1\Pi$ state has been already mentioned in Section 4B. It has a very flat minimum; nevertheless, it is bound by about 8 kcal/mol with $r_e \simeq$ 2.87 Å (see Figure 5).

E. States [(17, 33)$^1\Sigma^+$, $36^1\Sigma^-$, (2 repulsive)$^1\Pi$, $35^1\Delta$] and [(34, 39)$^3\Sigma^+$, $31^3\Sigma^-$, (25, 40)$^3\Pi$, $32^3\Delta$]. From the ground state of Al(^{2}P) and the second excited-state of N(^{2}P), we can construct 12 molecular AlN states, two of which of $^1\Pi$ symmetry are repulsive (see Figure 5). Their MRCI/A5Z ordering is shown in Figure 2.

The ground state ($17^1\Sigma^+$) of this 12-state manifold has a MRCI(+Q)/A5Z D_e = 47.5(51.3) kcal/mol and r_e = 1.812-(1.814) Å. It correlates to Al(^{2}P; M_L = 0) + N(^{2}P; M_L = 0), but an avoided crossing close to 7.5 bohr (see also Section 4D) changes its dominant equilibrium atomic character to Al(^{4}P; M_L = 0) + N(^{4}S) (Figure 4). It should also be mentioned that near 12 bohr the configurations of $17^1\Sigma^+$ and $33^1\Sigma^+$ start to mix; consequently, the equilibrium of the $17^1\Sigma^+$ carries a minor component of Al(^{2}P; $M_L = \pm 1$) + N(^{2}P; $M_L = \mp 1$).

The $33^1\Sigma^+$ displays two minima, a global (r_e^G = 2.819 Å) and a local (r_e^L = 1.692 Å), separated by a barrier of 18 kcal/mol with respect to the L-minimum. With respect to the G-minimum, the binding energy is 7.2 kcal/mol but is barely bound with respect to the L-minimum.

The $31^3\Sigma^-$ state displays two almost degenerate minima with an energy barrier of about 2.5 kcal/mol. The first minimum (r_e^G = 3.46 Å) interacts with the Rydberg-like $26^3\Sigma^-$ state, whereas the second (r_e^L = 2.37 Å) shows a mixed Rydberg and asymptotic Al(^{2}P; $M_L = \pm 1$) + N(^{2}P; $M_L = \mp 1$) character (Figure 7).

The $32^3\Delta$ state was already discussed in Section 4B. For numerical results, see Table 4, whereas its PEC is shown in Figure 7.

The $34^3\Sigma^+$ and $39^3\Sigma^+$ states correlate to Al($M_L = 0, \pm 1$) + N($M_L = 0, \mp 1$) channels, but they exchange their M_L values around 8.5 bohr due to an avoided crossing (Figure 6). The $34^3\Sigma^+$ state displays a van der Waals minimum of 1.0 kcal/mol; two more minima follow, a "G" and a "L" at r_e = 2.28 and 1.80 Å, respectively. The binding energy is 5.7(7.7) kcal/mol and the barrier height as measured from the L-minimum is 10 kcal/mol. Of course, the barrier is the result of an intense avoided crossing with the $39^3\Sigma^+$ state at 3.7 bohr. The latter, although overall repulsive, presents a well of 9.3 kcal/mol at 2.37 Å due to an avoided crossing near 5 bohr.

There is nothing much to be said about the $35^1\Delta$ state; it correlates to Al($M_L = \pm 1$) + N($M_L = \pm 1$) and is weakly bound: D_e = 4.6(7.3) kcal/mol at 2.58(2.54) Å (Figure 4).

The $36^1\Sigma^-$ state was first mentioned in Section 4B in conjunction with the $30^1\Sigma^-$ state. Its shallow minimum of 4 kcal/mol at 2.76 Å is the result of an avoided crossing with the $30^1\Sigma^-$ state (Figure 4).

The strong interaction among a series of $^3\Pi$ states including the 23, 25, and 40 states is manifested in the intensely irregular morphology of their PECs (Figure 8). The global minimum of the $25^3\Pi$ at r_e = 2.01 Å has a depth of 13.5 kcal/mol and corresponds to a binding energy of 16.3 kcal/mol with respect to Al(^{2}P) + N(^{2}P).

F. States $20^5\Delta$, $37^3\Delta$, (27, 38, 41)$^5\Sigma^-$. The two Δ-states above, $20^5\Delta$ (Figure 9) and $37^3\Delta$ (Figure 7), seems to correlate to the same end products, namely, Al(^{2}D; $M_L = \pm 2$) + N(^{4}S). Recall that the Al ^{2}D state is a mixture of $3s^23d^1$ and $3s^13p^2$ distributions (see Section 3). The $^5\Delta$ state has a smooth PEC with D_e = 51.6 kcal/mol and r_e = 1.833 Å. The $37^3\Delta$ state was first mentioned in Section 4B; it interacts with the $32^3\Delta$ at 4.2 bohr (Figure 7). Its PEC displays a rather shallow minimum at r_e = 1.994 Å and D_e = 8.2 kcal/mol.

The asymptotic products of 27 and $38^5\Sigma^-$ states are Al(^{2}D; M_L = 0) + N(^{4}S) and Al(^{2}P*; M_L = 0) + N(^{4}S), respectively; notice that the Al ^{2}P*($3s^24p^1$) state is of Rydberg character. Both states have been already discussed in Section 4C in conjunction with the $22^5\Sigma^-$ state (see also Figure 9). Finally, we cannot be certain of the end products of the $41^5\Sigma^-$ state, but some numerical results can be found in Table 4.

5. Summary and Remarks

For the diatomic AlN 45 states and their potential energy curves have been calculated at the MRCI/A5Z level of theory, spanning an energy range of 7 eV. For the two lowest $X^3\Pi$ and $A^3\Sigma^-$ states, core-correlation and scalar relativistic effects through second-order DKH approximation were taken into account. Concerning the ordering of the X and A states, our conclusion is that they are degenerate within the accuracy of our calculations, with a final energy difference ΔE(A $\rightarrow$ X) not larger than 1 kcal/mol. Therefore the spectroscopic symbols "X" and "A" are clearly formal. Because both of these states correlate to the same asymptotic fragments, Al(^{2}P) + N(^{4}S), it is also clear that their binding energies are practically the same although their bond distances differ by 0.13 Å. For the $X^3\Pi$ state our "recommended" D_0 and r_e values are 56.0 ± 0.5 kcal/mol and 1.783 Å, as contrasted to the experimental values 66 ± 9 kcal/mol and 1.7864 Å.

With the exception of the $X^3\Pi$ and $A^3\Sigma^-$ states, the ordering of the next five states is definitive: $a^1\Sigma^+$, $b^1\Pi$, $c^1\Delta$, $B^3\Sigma^+$, and $d^1\Sigma^+$. The $a^1\Sigma^+$ state features a triple bond, a bond distance r_e

= 1.682 Å (or shorter by about 0.01 Å if one correlates the Al $2s^2 2p^6$ electrons), and D_e = 102.1(103.5) kcal/mol at the MRCI-(+Q)/A5Z level, the largest D_e value of all states studied. The corresponding experimental dissociation energy of 78.62 kcal/mol is certainly in error.

In all 36 bound states, an average Mulliken charge transfer of about 0.3 e^- from Al to N is observed, perhaps as expected. The bonding is indeed complicated, and it is close to impossible to be deciphered for most of the states. However, in the $X^3\Pi$, $A^3\Sigma^-$, $a^1\Sigma^+$, $b^1\Pi$, $c^1\Delta$, and $B^3\Sigma^+$ states, the bonding comprises a single π bond, a single σ bond, a pure triple bond, a 1+1/2 π bond, a single σ bond, and 2 π bonds, respectively.

Finally, the present study shows the difficulties of obtaining definitive property values even for a "simple" diatomic as AlN with eight active electrons. The situation becomes more complex in the present case, because the first and the fourth excited states of Al are of Rydberg character, namely, $^2S^*(3s^2 4s^1)$ and $^2P^*(3s^2 4p^1)$, giving rise to three bound Rydberg molecular states (i.e., $22^5\Sigma^-$, $26^3\Sigma^-$, and $38^5\Sigma^-$).

Acknowledgment. The ample computing time made available to us by Professor T. H. Dunning, Jr., is greatly appreciated. This project is co-funded by the European Social Fund and National Resources (E.P.E.A.E.K. II) PYTHAGORAS (70/3/7373).

References and Notes

(1) Simmons, J. D.; McDonald, J. K. *J. Mol. Spectrosc.* **1972**, *41*, 584.
(2) Ebben, M.; ter Meulen, J. *J. Chem. Phys. Lett.* **1991**, *177*, 229.
(3) Pelissier, M.; Malrieu, J. P. *J. Mol. Spectrosc.* **1979**, *77*, 322.
(4) Langhoff, S. R.; Bauschlicher, C. W., Jr.; Pettersson, L. G. M. *J. Chem. Phys.* **1988**, *89*, 7354.
(5) Gutsev, G. L.; Jena, P.; Bartlett, R. J. *J. Chem. Phys.* **1999**, *110*, 2928.
(6) Clouthier, C. M.; Grein, F.; Bruna, P. J. *J. Mol. Spectrosc.* **2003**, *219*, 58.
(7) Grant, D. J.; Dixon, D. A. *J. Phys. Chem. A* **2005**, *109*, 10138.
(8) Gan, Z.; Grant, D. J.; Harrison, R. J.; Dixon, D. A. *J. Chem. Phys.* **2006**, *125*, 124311.
(9) (a) Nayak, S. K.; Khanna, S. N.; Jena, P. *Phys. Rev. B* **1998**, *57*, 3787. (b) Andrews, L.; Zhou, M.; Chertihin, G. V.; Bare, W. D.; Hannachi, Y. *J. Phys. Chem. A* **2000**, *104*, 1656. (c) Kandalam, A. K.; Pandey, R.; Blanco, M. A.; Costales, A., Recio, J. M.; Newsam, J. M. *J. Phys. Chem. B* **2000**, *104*, 4361. (d) Leskiw, B. D.; Castleman, A. D., Jr.; Ashman, C.; Khanna, S. N. *J. Chem. Phys.* **2001**, *114*, 1165. (e) Chang, Ch.; Patzer, A. B. C.; Sedlmayr, E.; Steinke, T.; Sülzle, D. *Chem. Phys.* **2001**, *271*, 283. (f) Jiang, Z.-Y.; Ma, W.-J.; Wu, H.-S.; Jin, Z.-H. *J. Mol. Struct. (THEOCHEM)* **2004**, *678*, 123.
(10) Meloni, G.; Gingerich, K. A. *J. Chem. Phys.* **2000**, *113*, 10978.
(11) Chase, M. W. *NIST-JANAF Thermochemical Tables*, 4th ed.; ACS, AIP, NSRDS: Gaithersburg, MD, 1998 (*J. Phys. Chem. Ref. Data*, Monograph 9).
(12) Stull, D. R.; Prophet, H. *JANAF Thermochemical Tables*, 2nd ed.; NSRDS-NBS 37; U.S. National Bureau of Standards: Washington, DC, 1971.
(13) Kalemos, A.; Dunning, T. H., Jr.; Mavridis, A. *J. Chem. Phys.* **2004**, *120*, 1813.
(14) Meloni, G.; Sheehan, S. M.; Parsons, B. F.; Newmark, D. M. *J. Phys. Chem. A* **2006**, *110*, 3527.
(15) (a) Dunning, T. H., Jr. *J. Chem. Phys.* **1989**, *90*, 1007. (b) Woon, D. E.; Dunning, T. H., Jr. *J. Chem. Phys.* **1993**, *98*, 1358.
(16) Peterson, K. A.; Dunning, T. H., Jr. *J. Chem. Phys.* **2002**, *117*, 10548.
(17) *MOLPRO* (2002.6) is a package of ab initio programs written by Werner, H.-J.; Knowles, P. J.; Lindh, R.; Manby, F. R.; Schütz, M.; Celani, P.; Korona, T.; Rauhut, G.; Amos, R. D.; Bernhardsson, A.; Berning, A.; Cooper, D. L.; Deegan, M. J. O.; Dobbyn, A. J.; Eckert, F.; Hampel, C.; Hetzer, G.; Lloyd, A. W.; McNicholas, S. J.; Meyer, W.; Mura, M. E.; Nicklass, A.; Palmieri, P.; Pitzer, R.; Schumann, U.; Stoll, H.; Stone, A. J.; Tarroni, R.; Thorsteinsson, T.
(18) (a) Douglas, M.; Kroll, N. M. *Ann. Phys.* **1974**, *82*, 89. (b) Hess, B. A. *Phys. Rev. A* **1985**, *32*, 756. (c) Hess, B. A. *Phys. Rev. A* **1986**, *33*, 3742. (d) Jansen, G.; Hess, B. A. *Phys. Rev. A* **1989**, *39*, 6016.
(19) (a) Boys, S. F.; Bernardi, F. *Mol. Phys.* **1970**, *19*, 553. (b) Liu, B.; McLean, A. D. *J. Chem. Phys.* **1973**, *59*, 4557. (c) Jansen, H. B.; Ros, P. *Chem. Phys. Lett.* **1969**, *3*, 140.
(20) Ralchenko, Yu.; Jou, F.-C.; Kelleher, D. E.; Kramida, A. E.; Musgrove, A.; Reader, J.; Wiese, W. L.; Olsen, K. *NIST Atomic Spectra Database* (version 3.1.0). 2006.
(21) Denis, P. A.; Balasubramanian, K. *Chem. Phys. Lett.* **2006**, *423*, 247.
(22) Theodorakopoulos, G.; Petsalakis, I. D. *Chem. Phys. Lett.* **2006**, *423*, 445.
(23) Lide, D. R., Ed. *CRC Handbook of Chemistry and Physics*, 72nd ed.; CRC Press: Boca Raton, FL, 1991.